

# On Adaptive Observer-based Control for Nonlinear Multiagent Systems: Event-triggered Strategies

Ziming Wang<sup>1</sup>, Yun Gao<sup>1</sup>, Apostolos I. Rikos<sup>2</sup>, Xin Wang<sup>3</sup>, and Yiding Ji<sup>1</sup>

**Abstract**—This paper explores the use of radial basis function neural networks (RBF NNs) and backstepping method to address the consensus tracking control problem in nonlinear semi-strict-feedback multiagent systems (MASs) that are affected by unknown states and perturbations. It introduces three different adaptive event-triggered control strategies, they are designed to compare controller update frequencies, thereby conserving scarce communication resources. To address the issues of unknown states and external perturbations detection while also reducing computational demands, a combined approach involving a state observer, a perturbation observer, and a first-order filter is proposed. In our analysis we establish that demonstrate that this method ensures all follower outputs can consistently track the leader's reference signal, while all error signals remaining uniformly bounded. Finally, we validate the efficiency of this control scheme through an illustrative example.

**Index Terms**—Multiagent system, adaptive control, observer, event-triggered control.

## I. INTRODUCTION

FOR decades, the synchronization challenge in nonlinear MASs has acquired significant interest from diverse academic fields due to its wide-ranging applications in areas such as power grids [1] [2], intelligent transportation [3] [4] and communication systems [5] [6]. The core intention of synchronization control is to ensure that all units within the network operate in harmony with a desired trajectory. Nevertheless, in many practical scenarios, system parameters are often uncertain and external perturbations unpredictable. This complicates achieving synchronization through conventional methods. Therefore, developing strategies to manage unknown states and perturbations holds considerable research importance.

In traditional sample-data control systems, the controller continuously responds to system changes, often leading to unnecessary resource use, especially with limited network bandwidth. A pivotal 1999 study [9] highlighted the advantages of event-triggered control (ETC) over periodic impulse control in first-order stochastic systems with multiplicative noise, leading to its widespread adoption in linear and nonlinear systems.

<sup>1</sup>Z. M. Wang, Y. Gao, and Y. D. Ji are with Robotics and Autonomous Systems Thrust of the System Hub, The Hong Kong University of Science and Technology (Guangzhou), Guangzhou, China. (e-mail: jiyyiding@hkust-gz.edu.cn).

<sup>2</sup>A. I. Rikos is with the Artificial Intelligence Thrust of the Information Hub, The Hong Kong University of Science and Technology (Guangzhou), Guangzhou, China.

<sup>3</sup>X. Wang is with the Chongqing Key Laboratory of Nonlinear Circuits and Intelligent Information Processing, College of Electronic and Information Engineering, Southwest University, Chongqing, China

Innovative design methodologies, as shown in [7]- [15] have greatly advanced ETC.

Initially, the event-triggered approach was effectively applied to nonlinear systems, as demonstrated in [7] and [8], reducing trigger frequency and enhancing controller utilization. Over time, researchers expanded this approach to various systems, introducing new trigger conditions. [7] proposed a simple dynamic triggering condition for easing traditional periodic execution requirements in closed-loop nonlinear systems, while [8] developed a technique using the plant's current state to determine timing, eliminating periodicity. Currently, many researchers are exploring event-triggered mechanisms in multi-agent systems (MASs). [10] suggested a saturated-threshold event-triggered control strategy for robust consensus tracking in sensor-attacked continuous-time nonlinear MASs, whereas [11] employed a switching-based triggered strategy for multi-agent consensus tracking. Notably, in 2016, [15] examined three event-triggered control strategies in nonlinear systems with uncertainty, without assuming input-to-state stability (ISS), prompting further investigation of this in MASs.

Motivated by the above information, we have developed an adaptive consensus tracking framework for high-order nonlinear MASs. Our approach utilizes the backstepping method, filter method, RBF NNs, and observer method. It is specifically designed for scenarios where the states and perturbations are unknown, while only the output signals of the agents are available. The key contributions of this work are outlined below:

- 1) Establishing state and perturbation observers can effectively monitor unmeasured states and perturbations, reducing the negative impacts of unmeasured factors. This enhances the controller's robustness against perturbations and introduces new challenges in observer design, making the controller more practical for real-world applications.
- 2) Unlike previous research [15] [16] [17], this study provides a comparative analysis of three event-triggered strategies: fixed-threshold, relative-threshold, and switch-threshold. The analysis effectively demonstrates their positive impacts. Each strategy uniquely reduces the frequency of control updates, thereby improving resource utilization and extending the controller's lifespan.

The organization of this paper is organized in the following way. Section II depicts the system model. The controller and event-triggered strategies are developed in Section III, while Section IV recommended the stability analysis. In Section V, we present our simulation results. Finally, we conclude the paper in Section VI.

## II. PRELIMINARIES

### A. Problem Formulation

Consider a scenario with  $M$  followers, designated as agents 1 to  $M$ , and a leader, designated as agent 0, all interacting under a directed communication graph topology. Consider the following class of MASs [20] [21]:

$$\begin{aligned}\dot{x}_{i,k} &= x_{i,k+1} + f_{i,k}(\bar{x}_{i,k}) + \xi_{i,k} \\ \dot{x}_{i,n} &= u_i + f_{i,n}(\bar{x}_{i,n}) + \xi_{i,n} \\ y_i &= x_{i,1}\end{aligned}\quad (1)$$

where  $i = 1, \dots, N$ ,  $j = 1, \dots, n$ ,  $k = 1, \dots, n-1$ ,  $\bar{x}_{i,j} = [x_{i,1}, \dots, x_{i,j}]^T$  are the state of the  $i$ th follower, while  $u_i \in R$  denotes its input of control. The output of the  $i$ th follower is expressed as  $y_i \in R$ . The function  $f_{i,j}(\bar{x}_{i,j})$  represents  $C^1$  class nonlinear smooth equation vectors.  $\xi_{i,j}$  represents unmeasured external perturbations affecting the system. It is noted that The leader's movement occurs independently, without being influenced by the actions or positions of the followers.

One intention of the works in this paper is to enable each follower's output signal,  $y_i$ , to synchronously track the reference signal,  $y_r$ , through a suitable ETC strategy.

### B. Observer Design

In this paper, to effectively spot the unknown states and perturbations throughout the entire control system, we introduce a series of observers. By precisely analyzing and processing feedback data, these observers can accurately identify and estimate unknown variables within the system, thereby enhancing the overall robustness and stability.

The state observer is defined as

$$\begin{aligned}\dot{\hat{x}}_{i,n} &= (P_i \otimes I_m) \dot{\hat{x}}_{i,n} + (Q_i \otimes y_i) + \sum_{l=1}^n (R_{i,l} \otimes \hat{f}_{i,l}(\dot{\hat{x}}_{i,l})) \\ &\quad + (U_i \otimes u_i) + \hat{\varpi}_i \\ y_i &= (V_i^T \otimes I_m) \hat{x}_n\end{aligned}\quad (2)$$

where  $\otimes$  represents the Kronecker product,  $\hat{x}_{i,l} = [\hat{x}_{i,1}^T, \dots, \hat{x}_{i,l}^T]^T$  represents the estimated value of the actual state. The vector  $Q_i = [q_{i,1}, \dots, q_{i,n}]^T$  is such that the matrix  $P_i$  is a strictly Hurwitz. The parameters are defined as

follows:  $R_{i,1} = \begin{bmatrix} 0, \dots, 1, \dots, 0 \end{bmatrix}_{n \times 1}^T$ ,  $U_i = [0, \dots, 0, 1]_{n \times 1}^T$ ,  
 $V_i = [1, 0, \dots, 0]_{n \times 1}^T$ ,  $P_i = \begin{bmatrix} -q_{i,1} \\ \vdots \\ I_{(n-1) \times (n-1)} \\ -q_{i,n} \ 0 \ \dots \ 0 \end{bmatrix}^T$ .

Define  $\psi_i = [(x_{i,1} - \hat{x}_{i,1})^T, \dots, (x_{i,n} - \hat{x}_{i,n})^T]^T$  as the error of state observation, one has that

$$\dot{\psi}_i = (P_i \otimes I_m) \psi_i + \tilde{\varpi}_i + \sum_{l=1}^n S_{i,l} \otimes (f_{i,l}(\bar{x}_{i,l}) - \hat{f}_{i,l}(\hat{x}_{i,l})) \quad (3)$$

Define  $\varphi_i(t) = \sum_{l=1}^n R_{i,l} \otimes (f_{i,l}(\bar{x}_{i,l}(t)) - \hat{f}_{i,l}(\hat{x}_{i,l}(t)))$  as the error of function approximation and  $\varphi_i(t) = [\varphi_{i,1}^T(t), \dots, \varphi_{i,n}^T(t)]^T$ , assume that  $\varphi_i(t)$  is bounded, this implies that there exists an unspecified parameter  $\varphi_i^0 > 0$  such that the inequality  $\|\varphi_i(t)\| \leq \varphi_i^0$  holds true.

By utilizing RBF NNs to approximate the unidentified nonlinear function within the MASs (1), an optimal weight vector  $W_{i,l}^*$  is defined as:

$$f_{i,l}(\bar{x}_{i,l}) = W_{i,l}^{*T} E_{i,l}(\hat{x}_{i,l}) + \sigma_{i,l}(t) \quad (4)$$

where  $\sigma_{i,l}(t)$  represents the bounded approximation error, i.e., there is a parameter  $\sigma_{0,l} > 0$  such that  $|\sigma_{i,l}(t)| \leq \sigma_{0,l}$ .

Consider  $\hat{W}_{i,l}^T$  as the estimation of  $W_{i,l}^{*T}$ , the unidentified smooth nonlinear function can be estimated as

$$\hat{f}_{i,l}(\hat{x}_{i,l}) = \hat{W}_{i,l}^T E_{i,l}(\hat{x}_{i,l}) \quad (5)$$

The optimal weight  $W_{i,l}^*$ , with  $l = 1, \dots, n$ , is designed as follows

$$W_{i,l}^* = \arg \min_{\hat{W}_{i,l} \in \tilde{\Omega}} \sup_{\substack{\bar{x}_{i,l} \in \Omega_{i,l} \\ \hat{x}_{i,l} \in \hat{\Omega}_{i,l}}} |\hat{f}_{i,l}(\hat{x}_{i,l}) - f(\bar{x}_{i,l})| \quad (6)$$

where  $\Omega_{i,l}$ ,  $\hat{\Omega}_{i,l}$  and  $\tilde{\Omega}$  represent compact sets corresponding to  $\bar{x}_{i,l}$ ,  $\hat{x}_{i,l}$ ,  $E_{i,l}$ . Besides, define  $\Theta_i^* = \max \{ \|W_{i,l}^*\| \}$ , where  $\hat{\Theta}_i$  represents the estimation of  $\Theta_i^*$  with  $\hat{\Theta}_i = \Theta_i^* - \hat{\Theta}_i$ .

The state observers can be revised as follows

$$\begin{aligned}\dot{\hat{x}}_{i,k} &= \hat{x}_{i,k+1} + \hat{W}_{i,k}^T E_{i,k}(\hat{x}_{i,k}) + q_{i,k} \psi_{i,1} + \hat{\varpi}_{i,k} \\ \dot{\hat{x}}_{i,n} &= u_i + \hat{W}_{i,n}^T E_{i,n}(\hat{x}_{i,n}) + q_{i,n} \psi_{i,1} + \hat{\varpi}_{i,n}\end{aligned}\quad (7)$$

with  $k = 1, \dots, n-1$ .

Define the estimate of external perturbations as  $\hat{\varpi}_i = [\hat{\varpi}_{i,1}^T, \dots, \hat{\varpi}_{i,n}^T]^T$ . and since the external perturbations are unknown, with the aim of achieving consensus control, a novel auxiliary variable is defined as

$$\tau_{i,l} = \varpi_{i,l} - \kappa_{i,l} x_{i,l} \quad (8)$$

where  $\kappa_{i,l}$  is a designed positive parameter.

The perturbation observer is designed as

$$\begin{aligned}\hat{\varpi}_{i,l} &= \hat{\tau}_{i,l} + \kappa_{i,l} \hat{x}_{i,l} \\ \dot{\hat{\tau}}_{i,l} &= -\kappa_{i,l} (\hat{W}_{i,l}^T E_{i,l}(\hat{x}_{i,l}) + \hat{\tau}_{i,l} + \kappa_{i,l} \hat{x}_{i,l} + \hat{x}_{i,l+1})\end{aligned}\quad (9)$$

where  $x_{i,n+1} = u_i$  and  $\hat{W}_{i,l}$  represents the estimation of  $W_{i,l}^*$ .

### C. Graph Theory

This article examines MASs comprising  $\mathcal{M}$  follower agents and one leaders. The interaction among these agents is represented using a directed graph  $\mathcal{G} = (\mathcal{V}, \mathcal{E})$ , where  $\mathcal{V}$  represents the set of nodes,  $\mathcal{V} = \{1, \dots, N\}$ , and  $\mathcal{E}$  represents the set of edges,  $\mathcal{E} \subseteq \mathcal{V} \times \mathcal{V}$ . By the way, the set  $\mathcal{E} = (\mathcal{V}_i, \mathcal{V}_j) \in \mathcal{E}$  means that agent  $j$  can gain information from agent  $i$ . The adjacent matrix  $\mathcal{A} = [a_{i,j}] \in R^{N \times N}$ , where

$$a_{i,j} = \begin{cases} 1, & \text{if } (\mathcal{V}_i, \mathcal{V}_j) \in \mathcal{E} \\ 0, & \text{if } (\mathcal{V}_i, \mathcal{V}_j) \notin \mathcal{E} \end{cases} \quad (10)$$

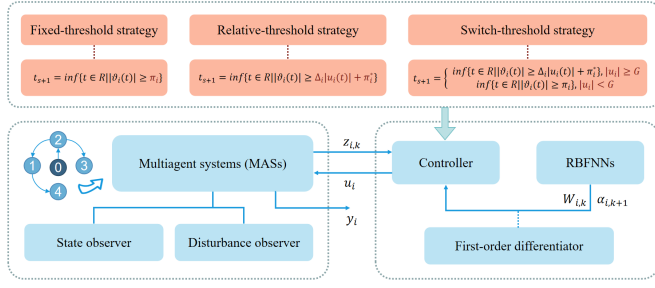


Fig. 1. Block diagram of the adaptive observer-based control with event-triggered strategies.

Define the Laplacian matrix  $\mathcal{L}$  as  $\mathcal{L} = \mathcal{D} - \mathcal{A}$ , where  $\mathcal{D} = \text{diag}(d_1, \dots, d_N)$  is defined as the in-degree matrix of graph  $\mathcal{G}$ ,  $d_i = \sum_{j=1, j \neq i}^N a_{ij}$ . And clarify the diagonal matrix  $\mathcal{B} = \text{diag}(\mathcal{C}_1, \dots, \mathcal{C}_N)$ , if the leader 0 is capable of transmitting information to agent  $i$ , then  $\mathcal{C}_i > 0$ . If not,  $\mathcal{C}_i = 0$  holds.

The previous section detailed the system setup process, while Fig. 1 presents the block diagram of the adaptive observer-based control framework with event-triggered strategies.

*Lemma 1* [18]: For any specified positive definite matrix  $H_i = H_i^T > 0$ , with a symmetric positive matrix  $F_i$ , the equality  $B_i^T F_i + F_i B_i = -2H_i$  holds.

*Lemma 2* [19]: The inequality  $0 \leq |\chi| - \chi \tanh(\frac{\chi}{\chi_0}) \leq 0.2785\chi_0$  always holds with any specified parameter  $\chi \in \mathbb{R}$  and  $\chi_0 > 0$ .

*Assumption 1* [20] : The unmeasured external perturbations are all bounded, i.e., the inequality  $\|\varpi_{i,j}\| \leq \varpi_{i,j}^0$  holds, where  $\varpi_{i,j}^0$  defines an positive parameter.

*Assumption 2* [21] : In this MASs, the leader's desired reference signal is both measurable and smooth, with  $y_r(t)$ ,  $\dot{y}_r(t)$  being bounded.

### III. THE CONTROLLER DESIGN

Define the graph-based errors  $z_{i,k}$  and the boundary layer errors  $e_{i,k}$  for the  $i$ th follower as

$$z_{i,1} = \sum_{j=1}^N a_{i,j} (y_i - y_j) + b_i (y_i - y_r) \quad (11)$$

$$z_{i,k} = x_{i,k} - \bar{\alpha}_{i,k} \quad (12)$$

$$e_{i,k} = \bar{\alpha}_{i,k} - \alpha_{i,k}$$

where  $k = 2, \dots, n$ . The terms  $\alpha_{i,k}$  and  $\bar{\alpha}_{i,k}$  respectively denote the virtual control and its filtered counterpart.

*Step 1*: The differential of  $z_{i,1}$  is

$$\dot{z}_{i,1} = (d_i + b_i) (\hat{x}_{i,2} + \psi_{i,2}(t) + \varpi_{i,1}(t) + f_{i,1}(\bar{x}_{i,1})) - b_i \dot{y}_r - \sum_{j=1}^N a_{i,j} (\hat{x}_{j,2} + \psi_{j,2}(t) + \varpi_{j,1}(t) + f_{j,1}(\bar{x}_{j,1})) \quad (13)$$

where  $d_i = \sum_{j=1}^N a_{ij}$ .

The Lyapunov function is determined as

$$V_{i,1} = \frac{z_{i,1}^2}{2} + \frac{\tilde{\tau}_{i,1}^2}{2} + \frac{1}{2\eta_{i,1}} \tilde{W}_{i,1}^T \tilde{W}_{i,1} + \frac{1}{2o_i} \tilde{\Theta}_i^2 + V_0$$

$$V_0 = \frac{1}{2} \psi_i^T (F_i \otimes I_m) \psi_i \quad (14)$$

where  $\psi_i = [\psi_{i,1}^T, \dots, \psi_{i,n}^T]^T$ ,  $\eta_{i,1} > 0$  and  $o_i > 0$  define designed parameters.

Define an auxiliary function as

$$\bar{Z}_{i,1}(T_{i,1}) = - \sum_{j=1}^N a_{i,j} (\hat{x}_{j,2} + f_{j,1}(\bar{x}_{j,1}) + \varpi_{j,1} + \psi_{j,2}) + (d_i + b_i) (f_{i,1}(\bar{x}_{i,1}) + \varpi_{i,1} + \psi_{i,2}) - b_i \dot{y}_r. \quad (15)$$

$\bar{Z}_{i,1}(T_{i,1})$  is estimated by RBF NNs:

$$\bar{Z}_{i,1}(T_{i,1}) = K_{i,1}^{*T} E_{i,1}(T_{i,1}) + \delta_{i,1}(T_{i,1}) \quad | \delta_{i,1}(T_{i,1}) | \leq \bar{\delta}_{i,1} \quad (16)$$

where  $\bar{\delta}_{i,1}$  defines an unknown positive parameter.

Based on the Young's inequality, the subsequent inequality can be derived:

$$z_{i,1} \bar{Z}_{i,1}(T_{i,1}) \leq \frac{\Theta_i^*}{2c_{i,1}^2} z_{i,1}^2 E_{i,1}^T(T_{i,1}) E_{i,1}(T_{i,1}) + \frac{c_{i,1}^2}{2} + \frac{z_{i,1}^2}{2} + \frac{\bar{\delta}_{i,1}^2}{2}. \quad (17)$$

where  $c_{i,1}$  is a positive designed parameter and  $T_{i,1} = [y_r, \dot{y}_r, \hat{x}_{i,1}^T, \hat{x}_{j,1}^T, \hat{\varpi}_{i,1}^T, \hat{\varpi}_{j,1}^T]^T$  denotes the input of RBF NNs.

In accordance with the Young's inequality and Assumption 1, one has

$$-\kappa_{i,1} \tilde{\tau}_{i,1} \sigma_{i,1} \leq \frac{1}{2} \tilde{\tau}_{i,1}^2 + \frac{\kappa_{i,1}^2 \sigma_{i,1}^2}{2} \quad (18)$$

$$-\kappa_{i,1} \tilde{\tau}_{i,1} \psi_{i,2} \leq \frac{1}{2} \tilde{\tau}_{i,1}^2 + \kappa_{i,1}^2 \|\psi_i\|^2 \quad (19)$$

$$-\kappa_{i,1}^2 \tilde{\tau}_{i,1} \psi_{i,1} \leq \frac{1}{2} \tilde{\tau}_{i,1}^2 + \kappa_{i,1}^4 \|\psi_i\|^2 \quad (20)$$

$$\psi_i^T (F_i \otimes I_m) \varphi_i \leq \frac{1}{2} \|F_i \otimes I_m\|^2 \|\varphi_i^0\|^2 + \frac{1}{2} \|\psi_i\|^2 \quad (21)$$

$$\psi_i^T (F_i \otimes I_m) \tilde{\varpi}_i \leq \frac{1}{2} \|F_i \otimes I_m\|^2 \|\tilde{\varpi}_i^0\|^2 + \frac{1}{2} \|\psi_i\|^2 \quad (22)$$

The design of the virtual control law and the adaptive law is formulated as

$$\alpha_{i,2} = \frac{1}{d_i + b_i} (r_{i,1} z_{i,1} - \frac{z_{i,1}}{2} - \frac{\hat{\Theta}_i}{2c_{i,1}^2} z_{i,1} E_{i,1}^T(T_{i,1}) E_{i,1}(T_{i,1})) \quad (23)$$

$$\dot{\hat{W}}_{i,1} = -h_{i,1} \hat{W}_{i,1} - \eta_{i,1} \tilde{\tau}_{i,1} \kappa_{i,1} E_{i,1}(\hat{x}_{i,1}) \quad (24)$$

where  $h_{i,1}$  and  $r_{i,1}$  are designed parameters.

Then, considering Lemma 1 and the above formulas, one has

$$\begin{aligned}\dot{V}_{i,1} \leq & r_{i,1} z_{i,1}^2 + (d_i + b_i) z_{i,1} (z_{i,2} + e_{i,2}) + \tilde{\tau}_{i,1} \tilde{\varpi}_{i,1} \\ & + \left( \frac{3 - 2\kappa_{i,1}}{2} \right) \tilde{\tau}_{i,1}^2 + \iota_{i,1} + \frac{h_{i,1}}{\eta_{i,1}} \tilde{W}_{i,1}^T \hat{W}_{i,1} \\ & + \tilde{\Theta}_i \left( \frac{1}{2c_{i,1}^2} z_{i,1}^2 E_{i,1}^T (T_{i,1}) E_{i,1} (T_{i,1}) - \frac{\dot{\Theta}_i}{o_i} \right) \\ & - \psi_i^T (H_i \otimes I_m) \psi_i + (1 + \kappa_{i,1}^2 + \kappa_{i,1}^4) \|\psi_i\|^2\end{aligned}\quad (25)$$

where  $\iota_{i,1} = \frac{c_{i,1}^2}{2} + \frac{\tilde{\delta}_{i,1}^2}{2} + \frac{\kappa_{i,1}^2 \sigma_{0,1}^2}{2} + \frac{1}{2} \|\varphi_i^0\|^2 \|F_i \otimes I_m\|^2 + \frac{1}{2} \|\tilde{\varpi}_i^0\|^2 \|F_i \otimes I_m\|^2$ .

Then, process  $\alpha_{i,2}$  through the first-order low-pass filter, resulting in  $\bar{\alpha}_{i,2}$  as follows:

$$\begin{aligned}\bar{\alpha}_{i,2}(0) &= \alpha_{i,2}(0) \\ m_{i,2} \dot{\bar{\alpha}}_{i,2} + \bar{\alpha}_{i,2} &= \alpha_{i,2}\end{aligned}\quad (26)$$

where  $m_{i,2}$  is a small positive designed parameter.

Step k: Differentiating  $z_{i,k}$ , one has

$$\begin{aligned}\dot{z}_{i,k} = & z_{i,k+1} + s_{i,k+1} + \hat{W}_{i,k}^T E_{i,k} (\hat{x}_{i,k}) + q_{i,k} \psi_{i,1} \\ & + \hat{\varpi}_{i,k}(t) + \alpha_{i,k+1} - \dot{\bar{\alpha}}_{i,k}\end{aligned}\quad (27)$$

where  $k = 2, \dots, n-1$ .

Choose the Lyapunov function as

$$V_{i,k} = \frac{z_{i,k}^2}{2} + \frac{\tilde{\tau}_{i,k}^2}{2} + \frac{1}{2\eta_{i,k}} \tilde{W}_{i,k}^T \tilde{W}_{i,k}\quad (28)$$

where  $\eta_{i,k}$  is a positive parameter.

By utilizing RBF NNs, one has

$$\begin{aligned}\bar{Z}_{i,k}(T_{i,k}) = & K_{i,k}^{*T} E_{i,k}(T_{i,k}) + \delta_{i,k}(T_{i,k}) \\ |\delta_{i,k}(T_{i,k})| \leq & \bar{\delta}_{i,k}\end{aligned}\quad (29)$$

where  $\bar{\delta}_{i,k}$  denotes an unknown positive parameter.

The design of the virtual control law and the adaptive law is formulated as follows

$$\begin{aligned}\alpha_{i,k+1} = & r_{i,k} z_{i,k} - \frac{z_{i,k}}{2} + \frac{\alpha_{i,k} - \bar{\alpha}_{i,k}}{m_{i,k}} - q_{i,k} \psi_{i,1} \\ & - \frac{\dot{\Theta}_i}{2c_{i,k}^2} z_{i,k} E_{i,k}^T (T_{i,k}) E_{i,k} (T_{i,k})\end{aligned}\quad (30)$$

$$\dot{\tilde{W}}_{i,k} = -h_{i,k} \hat{W}_{i,k} - \eta_{i,k} \tilde{\tau}_{i,k} \kappa_{i,k} E_{i,k} (\hat{x}_{i,k})\quad (31)$$

where  $T_{i,k} = [y_r, \hat{\Theta}_i, \hat{x}_{i,k}^T, \hat{x}_{j,k}^T, \hat{\varpi}_{i,k}^T, \hat{\varpi}_{j,k}^T]^T$ ,  $r_{i,k}$  and  $h_{i,k}$  are designed parameters.

In terms of the Young's inequality, one has

$$\begin{aligned}\dot{V}_{i,k} \leq & r_{i,k} z_{i,k}^2 + (\kappa_{i,k}^2 + \kappa_{i,k}^4) \|\psi_i\|^2 + z_{i,k} (z_{i,k+1} + e_{i,k+1}) \\ & + \frac{h_{i,k}}{\eta_{i,k}} \tilde{W}_{i,k}^T \hat{W}_{i,k} + \left( \frac{3 - 2\kappa_{i,k}}{2} \right) \tilde{\tau}_{i,k}^2 + \tilde{\tau}_{i,k} \dot{\tilde{\varpi}}_{i,k} \\ & + \frac{\dot{\Theta}_i}{2c_{i,k}^2} z_{i,k}^2 E_{i,k}^T (T_{i,k}) E_{i,k} (T_{i,k}) + \iota_{i,k}\end{aligned}\quad (32)$$

where  $\iota_{i,k} = \frac{c_{i,k}^2}{2} + \frac{\tilde{\delta}_{i,k}^2}{2} + \frac{\kappa_{i,k}^2 \sigma_{0,k}^2}{2}$ , and  $c_{i,k}$  denotes a positive parameter.

In line with Step 1, the first-order low-pass filter is implemented as follows:

$$\begin{aligned}\bar{\alpha}_{i,k+1}(0) &= \alpha_{i,k+1}(0) \\ m_{i,k+1} \dot{\bar{\alpha}}_{i,k+1} + \bar{\alpha}_{i,k+1} &= \alpha_{i,k+1}.\end{aligned}\quad (33)$$

where  $m_{i,k+1}$  denotes a slight positive designed parameter.

Step n: Differentiating  $z_{i,n}$ , one gets

$$\dot{z}_{i,n} = u_i + \hat{W}_{i,n}^T E_{i,n} (\hat{x}_{i,n}) + q_{i,n} \psi_{i,1} + \hat{\varpi}_{i,n}(t) - \dot{\bar{\alpha}}_{i,n}\quad (34)$$

Choose the Lyapunov function as

$$V_{i,n} = \frac{z_{i,n}^2}{2} + \frac{\tilde{\tau}_{i,n}^2}{2} + \frac{1}{2\eta_{i,n}} \tilde{W}_{i,n}^T \tilde{W}_{i,n}\quad (35)$$

where  $\eta_{i,n}$  denotes a designed positive parameter.

By utilizing RBF NNs, one has

$$\begin{aligned}\bar{Z}_{i,n}(T_{i,n}) = & K_{i,n}^{*T} E_{i,n}(T_{i,n}) + \delta_{i,n}(T_{i,n}) \\ |\delta_{i,n}(T_{i,n})| \leq & \bar{\delta}_{i,n}\end{aligned}\quad (36)$$

where  $\bar{\delta}_{i,n}$  denotes an unknown positive parameter.

The control law and adaptive parameters are constructed as

$$\begin{aligned}\alpha_{i,n+1} = & r_{i,n} z_{i,n} - \frac{z_{i,n}}{2} + \frac{\alpha_{i,n} - \bar{\alpha}_{i,n}}{m_{i,n}} - q_{i,n} \psi_{i,1} \\ & - \frac{\dot{\Theta}_i}{2c_{i,n}^2} z_{i,n} E_{i,n}^T (T_{i,n}) E_{i,n} (T_{i,n})\end{aligned}\quad (37)$$

$$\dot{\tilde{W}}_{i,n} = -h_{i,n} \hat{W}_{i,n} - \eta_{i,n} \tilde{\tau}_{i,n} \kappa_{i,n} E_{i,n} (\hat{x}_{i,n})\quad (38)$$

$$\dot{\bar{\alpha}}_{i,n} = -\lambda_i \dot{\Theta}_i + \sum_{k=1}^n \frac{o_i}{2c_{i,k}^2} z_{i,k}^2 E_{i,k}^T (T_{i,k}) E_{i,k} (T_{i,k})\quad (39)$$

where  $r_{i,n}$ ,  $h_{i,n}$  and  $\lambda_i$  are designed parameters.

#### A. Fixed-threshold strategy

In this strategy, the adaptive event-triggered controller is reformulated as

$$w_i(t) = \alpha_{i,n+1} - \bar{\pi}_i \tanh\left(\frac{z_{i,n} \bar{\pi}_i}{\mu_i}\right)\quad (40)$$

The triggering condition is defined as

$$u_i(t) = w_i(t_s), \quad \forall t \in [t_s, t_{s+1})\quad (41)$$

$$t_{s+1} = \inf \{t \in R \mid |\vartheta_i(t)| \geq \pi_i\}, \quad t_1 = 0\quad (42)$$

where  $\vartheta_i(t) = w_i(t) - u_i(t)$  represents the measurement-triggered error, while  $t_s$  indicates the controller's update time, with  $s \in \mathbb{Z}$ . The parameters  $\bar{\pi}_i$ ,  $\pi_i$  and  $\mu_i$  are designed and positive,  $\bar{\pi} > \pi_i$ . The control signal  $u_i(t_{s+1})$  is applied to the system when condition (42) is activated. During the interval  $t \in [t_s, t_{s+1})$ , i.e.  $|\vartheta_i(t) - u_i(t)| < \pi_i$ , the controller maintains a constant value of  $w_i(t_s)$ . For a function  $\epsilon_i(t)$  that changes continuously over time that satisfies  $\epsilon_i(t_s) = 0$  and  $\epsilon_i(t_{s+1}) = \pm 1$  with  $|\epsilon_i(t)| \leq 1$ , it follows that  $w_i(t) = u_i(t) + \epsilon_i(t)$ .

Based on Lemma 2, the inequality  $-\epsilon_i(t)\pi_i z_{i,n} - \bar{\pi}_i z_{i,n} \tanh(\frac{z_{i,n}\bar{\pi}_i}{\mu_i}) \leq 0.2875\mu_i$  holds, then, differentiate  $\dot{V}_{i,n}$  by utilizing the Young's inequality and (36)-(38), one gets

$$\begin{aligned} \dot{V}_{i,n} \leq & r_{i,n} z_{i,n}^2 + \left(\frac{3-2\kappa_{i,n}}{2}\right) \tilde{\tau}_{i,n}^2 + \tilde{\tau}_{i,n} \dot{\varpi}_{i,n} \\ & + \frac{\tilde{\Theta}_i}{2c_{i,n}^2} z_{i,n}^2 E_{i,n}^T (T_{i,n}) E_{i,n} (T_{i,n}) + \iota_{i,n} \\ & + \frac{h_{i,n}}{\eta_{i,n}} \tilde{W}_{i,n}^T \hat{W}_{i,n} + (\kappa_{i,n}^2 + \kappa_{i,n}^4) \|\psi_i\|^2 \end{aligned} \quad (43)$$

where  $\iota_{i,n} = \frac{c_{i,n}^2}{2} + \frac{\delta_{i,n}^2}{2} + \frac{\kappa_{i,n}^2 \sigma_{0,n}^2}{2} + 0.2785\mu_i$ ,  $c_{i,n}$  is a positive parameter.

### B. Relative-threshold strategy

In the fixed-threshold strategy, it is observed that the threshold  $\pi_i$  remains constant regardless of the control signal's magnitude. Nevertheless, when addressing a stabilization problem, adopting a variable threshold for the triggering condition becomes advantageous, according to the approach in [22] [23]. Specifically, when the control signal  $u_i$  is huge, a greater error of measurement can be tolerated, allowing for longer update intervals. Conversely, as the system states stabilize towards equilibrium, with  $u_i$  approaching zero, a smaller threshold enables more accurate control, enhancing overall system performance. Then, it is proposed the following adaptive event-triggered controller:

$$\begin{aligned} w_i(t) = & -(1 + \Delta_i)(\alpha_{i,n+1} \tanh(\frac{z_{i,n}\alpha_{i,n+1}}{\mu_i}) \\ & + \bar{\pi}_i^* \tanh(\frac{z_{i,n}\bar{\pi}_i^*}{\mu_i})) \end{aligned} \quad (44)$$

The triggering condition is defined as

$$u_i(t) = w_i(t_s), \quad \forall t \in [t_s, t_{s+1}] \quad (45)$$

$$t_{s+1} = \inf \{t \in R | |\vartheta_i(t)| \geq \Delta_i |u_i(t)| + \pi_i^*\} \quad (46)$$

where  $t_s$  represents the time when the controller is updated,  $s \in Z$ ,  $\mu_i$ ,  $\Delta_i$ ,  $0 < \Delta_i < 1$ ,  $\pi_i^* > 0$ , and  $\bar{\pi}_i^* > \pi_i^*/(1 - \Delta_i)$  are all positive designed parameters.

From (49), we have  $w_i(t) = (1 + \rho_{1,i}(t))u_i(t) + \rho_{2,i}(t)\pi_i^*$  in the interval  $[t_s, t_{s+1}]$ , where  $\rho_{1,i}(t)$  and  $\rho_{2,i}(t)$  denote time-varying parameters satisfying  $|\rho_{1,i}(t)| \leq 1$  and  $|\rho_{2,i}(t)| \leq 1$ .

Thus, one has

$$u_i(t) = \frac{w_i(t)}{1 + \rho_{1,i}(t)\Delta_i} - \frac{\rho_{2,i}(t)\pi_i^*}{1 + \rho_{1,i}(t)\Delta_i} \quad (47)$$

Since  $\forall a_i \in R$  and  $\mu_i > 0$ , from (45) we get  $z_{i,n}w_i(t) \leq 0$ , one has

$$\frac{z_{i,n}w_i(t)}{1 + \rho_{1,i}(t)\Delta_i} \leq \frac{z_{i,n}w_i(t)}{1 + \Delta_i} \quad (48)$$

$$\frac{\rho_{2,i}\pi_i^*}{1 + \rho_{1,i}(t)\Delta_i} \leq \frac{\pi_i^*}{1 - \Delta_i} \quad (49)$$

According to the above analysis, similar to (43), it can be obtained the same derivative result of  $\dot{V}_{i,n}$  with different  $\iota_{i,n}$ , where  $\iota_{i,n} = \frac{c_{i,n}^2}{2} + \frac{\delta_{i,n}^2}{2} + \frac{\kappa_{i,n}^2 \sigma_{0,n}^2}{2} + 0.557\mu_i$ .

### C. Switch-threshold strategy

In this portion, it is introduced a switch-threshold strategy. The relative-threshold approach adjusts the threshold based on the control signal's magnitude, allowing for longer update intervals when the signal is huge and more precise control as the signal nears zero, thus improving performance. However, a very large control signal can lead to significant measurement errors and abrupt changes during updates. In contrast, the fixed-threshold strategy maintains a consistent upper limit on measurement errors, regardless of signal size. Considering these aspects, we propose the following switched-threshold strategy. The triggering condition is defined as follows:

$$u_i(t) = w_i(t_s), \quad \forall t \in [t_s, t_{s+1}] \quad (50)$$

$$t_{s+1} = \begin{cases} \inf \{t \in R | |\vartheta_i(t)| \geq \Delta_i |u_i(t)| + \pi_i^* \}, |u_i| \geq G \\ \inf \{t \in R | |\vartheta_i(t)| \geq \pi_i \}, |u_i| < G \end{cases} \quad (51)$$

where  $G$  is the designed switching gate.

For this switch-threshold strategy, one has

$$\bar{\vartheta}_i = \sup |\vartheta_i(t)| \leq \max \{(\Delta_i |u_i(t)| + \pi_i^*), \pi_i\} \quad (52)$$

where  $t \in [t_s, t_{s+1}]$ .

Since the switch-threshold strategy employs an identical control law to both the fixed-threshold and relative-threshold strategies, the ultimate bounds for tracking and stabilization errors remain consistent with those of the two previously mentioned strategies.

## IV. STABILITY ANALYSIS

Considering the previous analysis, we have developed observers and designed an adaptive consensus tracking controller via RBF NNs, backstepping method and three event-triggered strategies. In this section, we demonstrate the boundedness of all signals by employing Lyapunov stability theory. In addition, the event-triggered strategies are proven to be effective, and the Zeno behavior is avoided.

*Theorem 1:* For the nonlinear MASs in equation (1) with the event-triggered controllers in equation (40)-(44), if the initial condition satisfies  $V(0) \leq \Omega$ , the error signals  $z_{i,k}$ ,  $\tilde{c}_{i,k}$ ,  $\tilde{W}_{i,k}$ ,  $\tilde{\Theta}_i$ ,  $e_{i,k}$ , and  $\psi_{i,k}$  are all uniformly bounded. Furthermore, the errors of consensus tracking between the followers' outputs and the leader's trajectory signal can be minimized to a specified range.

*Proof:* See Appendix A.

## V. ILLUSTRATIVE EXAMPLE

This section will examine an illustrative example to validate the performance and effectiveness of the proposed approach. The system comprises one leader agent and four follower agents. The dynamics of each agent are described by:

$$\begin{aligned} \dot{x}_{i,1} &= x_{i,2} + f_{i,1}(\bar{x}_{i,1}) + \xi_{i,1} \\ \dot{x}_{i,2} &= u_i + f_{i,2}(\bar{x}_{i,2}) + \xi_{i,2} \\ y_i(t) &= x_{i,1} \end{aligned} \quad (53)$$

where  $f_{i,1}(\bar{x}_{i,1}) = 0.8x_{i,1}e^{-1.4x_{i,2}^2}$ ,  $f_{i,2}(\bar{x}_{i,2}) = -0.5x_{i,1}^2 \cos(x_{i,2})$ ,  $\xi_{i,1} = 0.8x_{i,1} \sin(x_{i,2}) \cos^2(t)$  and

$\xi_{i,2} = 0.2x_{i,2} \cos(x_{i,1}) \cos^2(t)$ ,  $i = 1, \dots, 4$ . The leader's trajectory signal is defined as  $y_r = -0.5 \sin(4t) \cos(2t)$ .

The communication topology is illustrated in Fig. 1. The connection matrix linking the leader to the followers is represented as  $\mathcal{B} = \text{diag}\{0, 1, 0, 0\}$ . And the adjacency matrix  $\mathcal{A}$  and the Laplacian matrix  $\mathcal{L}$  are presented as follows:

$$\mathcal{A} = \begin{bmatrix} 0 & 1 & 0 & 0 \\ 0 & 0 & 0 & 0 \\ 0 & 1 & 0 & 0 \\ 1 & 0 & 0 & 0 \end{bmatrix}, \mathcal{L} = \begin{bmatrix} 1 & -1 & 0 & 0 \\ 0 & 0 & 0 & 0 \\ 0 & -1 & 1 & 0 \\ -1 & 0 & 0 & 1 \end{bmatrix}.$$

The initial conditions of the four followers and state observers are selected as follows:

$$\begin{array}{ll} \bar{x}_{1,2}(0) = [0.2, 0]^T & \hat{x}_{1,2}(0) = [0.3, 1.7]^T \\ \bar{x}_{2,2}(0) = [-0.2, 0]^T & \hat{x}_{2,2}(0) = [-0.5, 1.7]^T \\ \bar{x}_{3,2}(0) = [0.1, 0]^T & \hat{x}_{3,2}(0) = [0, -4]^T \\ \bar{x}_{4,2}(0) = [-0.3, 0]^T & \hat{x}_{4,2}(0) = [0, -4]^T \end{array}$$

Based on the parameter selection guidelines outlined in the stability analysis, the quantitative values of the design parameters are as follows: for fix-threshold strategy,  $\pi_i = 2.5$ ,  $\bar{\pi}_i = 4$ ,  $\mu_i = 5.4$ , for relative-threshold strategy,  $\pi_i^* = 2$ ,  $\bar{\pi}_i^* = 4$ ,  $\Delta_i = 0.245$ , for switch-threshold strategy  $G = 6$ , for the first order low pass filter,  $m_i = 0.005$ , for other parameters,  $h_{i,1} = h_{i,2} = 50$ ,  $r_{i,1} = r_{i,2} = -100$ ,  $c_{i,1} = c_{i,2} = 100$ ,  $\eta_{i,1} = \eta_{i,2} = 0.01$ ,  $q_{i,1} = 350$ ,  $q_{i,2} = 0.5$ ,  $\lambda_i = 120$  and  $\alpha_i = 25$ .

In Fig. 2, shortly after the process begins, all followers within the system consistently follow the leader, successfully achieving the adaptive consensus control objective. Fig. 3 is presented to illustrate that the tracking error has converged to zero. The total triggering number for sample-data strategy is 5,000 times, and the triggering numbers for the three threshold strategies are detailed in Table I. Figs. 4 shows that the interval of events respectively triggered by three strategies. According to the statistics, it is clear that under the fixed-threshold strategy, the number of triggers is the highest. Under the relative-threshold strategy, the number of triggers is the lowest, while under the switch-threshold strategy, the number of triggers falls and both types of triggers play an indispensable role in this strategy.

TABLE I  
COMPARISON OF THREE EVENT-TRIGGERED STRATEGIES.

	Fixed-threshold	Switch-threshold	Relative-threshold
Follower 1	364	344(255 + 89)	310
Follower 2	296	281(220 + 61)	277
Follower 3	358	342(255 + 87)	308
Follower 4	453	420(306 + 114)	380

*Remark 1:* The theoretical analysis and simulation results indicate that the fixed-threshold strategy maintains bounded measurement error regardless of control amplitude, reducing the risk of excessive control signals that could impair system performance. In contrast, the relative-threshold strategy adjusts controller update intervals based on control amplitude variations, minimizing control actions while maintaining tracking performance, thereby extending controller lifespan and improving resource utilization. The switch-threshold strategy

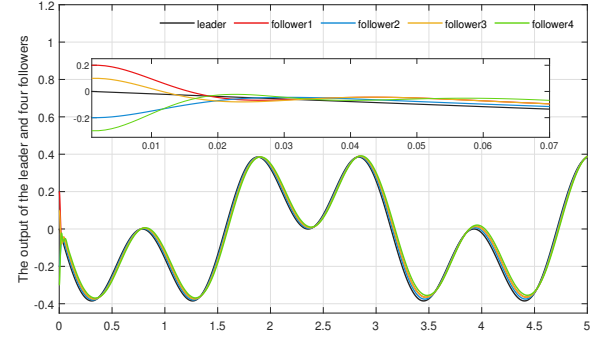


Fig. 2. Consensus tracking performance.

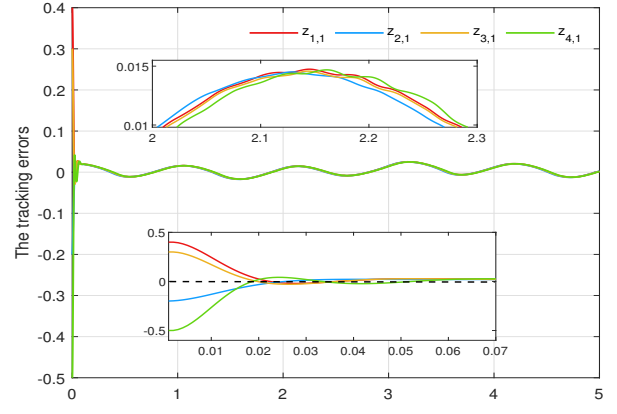


Fig. 3. Trajectories of tracking errors  $z_{i,1}$  ( $i = 1, 2, 3, 4$ ).

combines the benefits of both approaches by regulating trigger occurrences at an intermediate level, adjusting activation frequency through a designed switching gate.

## VI. CONCLUSION

This article addresses the observer-based consensus tracking issue for nonlinear MASs via three event-triggered control strategies. The RBF NNs are utilized to estimate unidentified nonlinear functions, while observers handle unmeasurable states and unknown perturbations. Complexity is managed by incorporating a filter at each design step. Furthermore, by comprising three event-triggered strategies, Besides, three distinct strategies for controller updates are presented. Simulation results indicate that the proposed Fixed-threshold strategy can better ensure system performance while reducing the number of triggering instances. Relative-threshold strategy minimizes the number of triggering instances to conserve resources. Switch-threshold strategy effectively balances system performance with resource utilization for each agent. Future work will focus on the optimized event-triggered control for stochastic nonlinear MASs.

## ACKNOWLEDGMENT

The authors wish to convey their appreciation to Ning Pang at Shanghai Jiao Tong University for insightful

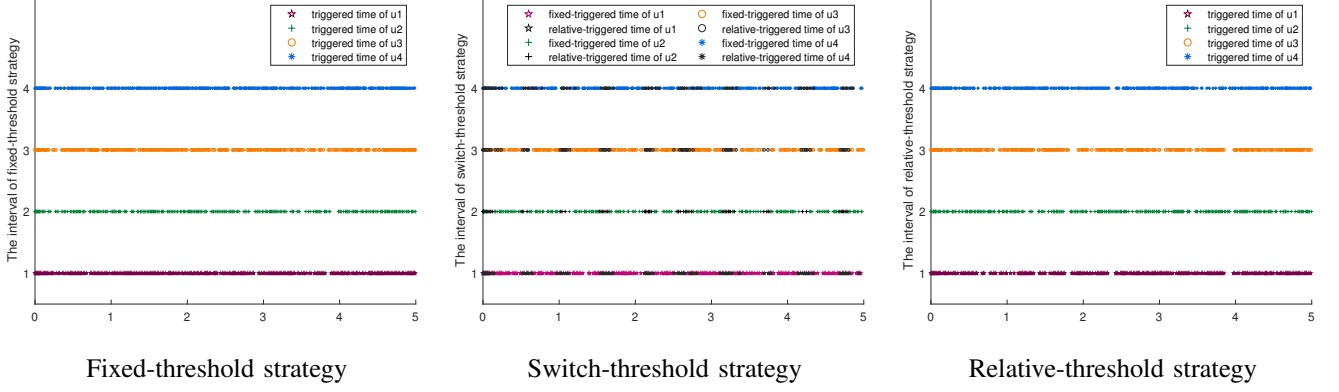


Fig. 4. Event-triggered release instants and interval: three strategies.

discussions about some of the issues addressed in this paper. This work is partially supported by the National Natural Science Foundation of China under grants 62303389 and 62373289, Guangdong Basic and Applied Basic Research Funding under grants 2022A151511076 and 2024A1515012586, Guangzhou Basic and Applied Basic Research Scheme under grants 2023A04J1067, together with Guangzhou-HKUST(GZ) Joint Funding Program under grants 2023A03J0678, 2023A03J0011, 2024A03J0618 and 2024A03J0680.

## APPENDIX

### PROOF OF THEOREM 1

Define the following  $i = 1, \dots, N$  and the overall Lyapunov function for the MAsSs (1) as

$$V = \sum_{i=1}^N \sum_{k=1}^n V_{i,k} + \sum_{i=1}^N \sum_{k=1}^{n-1} \frac{e_{i,k+1}^2}{2} \quad (54)$$

Based on the Young's inequality, one gets

$$z_{i,1} (z_{i,2} + e_{i,2}) \leq z_{i,1}^2 + \frac{1}{2} z_{i,2}^2 + \frac{1}{2} e_{i,2}^2 \quad (55)$$

$$\tilde{E}_{i,k}^T \dot{E}_{i,k} \leq -\frac{1}{2} \tilde{E}_{i,k}^T \tilde{E}_{i,k} + \frac{1}{2} E_{i,k}^{*T} E_{i,k}^* \quad (56)$$

$$\tilde{\Theta}_i \tilde{\Theta}_i \leq \frac{1}{2} (\Theta_i^*)^2 - \frac{1}{2} \tilde{\Theta}_i^2. \quad (57)$$

Define the parameters  $r_{i,1}$ ,  $r_{i,2}$ ,  $r_{i,k}$  and  $r_{i,n}$  as  $r_{i,1} = -(d_i + b_i) + r_{i,1}^*$ ,  $r_{i,2} = -\frac{d_i + b_i}{2} - 1 + r_{i,2}^*$ ,  $r_{i,k} = -\frac{3}{2} + r_{i,k}^*$  and  $r_{i,n} = -\frac{1}{2} + r_{i,n}^*$  with  $k = 3, \dots, n-1$ .

While  $\|\dot{\tilde{\psi}}_{i,k}\| \leq \kappa_{i,k}^* \|\tilde{\tau}_{i,k}\|$ , one has

$$\begin{aligned} \dot{V} \leq & \sum_{i=1}^N \left\{ \sum_{k=1}^n r_{i,k}^* z_{i,k}^2 + \sum_{k=2}^{n-1} \frac{e_{i,k+1}^2}{2} + \frac{d_i + b_i}{2} e_{i,2}^2 \right. \\ & + \sum_{k=1}^{n-1} e_{i,k+1} \dot{e}_{i,k+1} + 2 \sum_{k=1}^n \kappa_{i,k}^* \tilde{\tau}_{i,k}^2 + \frac{\lambda_i}{2o_i} (\Theta_i^{*2} - \tilde{\Theta}_i^2) \\ & + \sum_{k=1}^n \frac{h_{i,k}}{2\eta_{i,k}} (W_{i,k}^{*T} W_{i,k}^* - \tilde{W}_{i,k}^T \tilde{W}_{i,k}) + \sum_{k=1}^n \iota_{i,k} \\ & \left. - \psi_i^T ((H_i - (1 + \sum_{k=1}^n (\kappa_{i,k}^2 + \kappa_{i,k}^4)) I_n) \otimes I_m) \psi_i \right\} \end{aligned} \quad (58)$$

where  $\kappa_{i,k}^* = (3 - 2\kappa_{i,k})/2$ ,  $r_{i,k}^*$  and  $\kappa_{i,k}^*$  denote unmeasured parameters for stability analysis, with  $k = 1, \dots, n$ .

$\hbar(\bullet)$  is defined as the eigenvalue of the given matrix. Select the matrix  $H_i$  such that  $\hbar_{\min}[H_i - (1 + \sum_{k=1}^n (\kappa_{i,k}^2 + \kappa_{i,k}^4)) I_n] = \wp_i / 2\hbar_{\max}(F_i)$ , where  $\wp_i$  denotes a positive parameter.

Differentiate with respect to time of  $e_{i,2}$  and  $e_{i,k+1}$ , one has

$$\begin{aligned} \dot{e}_{i,2} &= -\frac{e_{i,2}}{m_{i,2}} + \Gamma_{i,2} \\ \dot{e}_{i,k+1} &= -\frac{e_{i,k+1}}{m_{i,k+1}} + \Gamma_{i,k+1} \end{aligned} \quad (59)$$

where  $\Gamma_{i,2}$  and  $\Gamma_{i,k+1}$  can be represented as  $\Gamma_{i,2} = -\frac{r_{i,1} \dot{z}_{i,1}}{d_i + b_i} + \frac{\dot{\Theta}_i}{2c_{i,1}^2(d_i + b_i)} \dot{z}_{i,1} E_{i,1}^T (T_{i,1}) E_{i,1} (T_{i,1}) + \frac{\dot{z}_{i,1}}{2(d_i + b_i)} + \frac{\dot{\Theta}_i}{c_{i,1}^2(d_i + b_i)} z_{i,1} E_{i,1}^T (T_{i,1}) \dot{E}_{i,1} (T_{i,1})$  and  $\Gamma_{i,k+1} = \frac{\dot{e}_{i,k}}{m_{i,k}} + q_{i,k} \dot{\psi}_{i,1} + \frac{\dot{\Theta}_i}{2c_{i,k}^2} \dot{z}_{i,k} E_{i,k}^T (T_{i,k}) E_{i,k} (T_{i,k}) - r_{i,k} \dot{z}_{i,k} + \frac{\dot{z}_{i,k}}{2} + \frac{\dot{\Theta}_i}{c_{i,k}^2} z_{i,k} E_{i,k}^T (T_{i,k}) \dot{E}_{i,k} (T_{i,k})$ .

Inspired by the work presented in [21], we analyze the sets

$$\begin{aligned} \mathbb{M}_{i,k} = & \left\{ \sum_{i=1}^N \sum_{k=1}^n (z_{i,k}^2 + \tilde{\tau}_{i,k}^2 + \frac{1}{\eta_{i,k}} \tilde{W}_{i,k}^T \tilde{W}_{i,k}) + \sum_{i=1}^N \frac{1}{o_i} \tilde{\Theta}_i^2 \right. \\ & \left. + \sum_{i=1}^N \psi_i^T (F_i \otimes I_m) \psi_i + \sum_{i=1}^N \sum_{k=1}^{n-1} e_{i,k+1}^2 \leq 2\Omega \right\} \end{aligned} \quad (60)$$

where  $\mathbb{M}_{i,k}$  is compact in  $R^{\dim(\mathbb{C}_{i,k})}$ , there exists an inequality  $\|\Gamma_{i,k+1}\| \leq L_{i,k+1}$ , where  $L_{i,k+1}$  denotes a positive parameter.

Applying the Young's inequality, one can get  $\Gamma_{i,k+1} e_{i,k+1} \leq \frac{\Xi}{2} + \frac{L_{i,k+1} e_{i,k+1}^2}{2\Xi}$ , where  $\Xi$  is a positive parameter, with  $k = 1, \dots, n-1$ .

Select the parameters as  $\frac{1}{m_{i,2}} = \frac{d_i + b_i}{2} + \frac{L_{i,2}^2}{2\Xi} + m_{i,2}^*$  and  $\frac{1}{m_{i,k+1}} = \frac{1}{2} + \frac{L_{i,k+1}^2}{2\Xi} + m_{i,k+1}^*$ , where  $m_{i,k+1}^*$  denotes an unknown positive parameter, with  $k = 2, \dots, n-1$ .

With  $l = 2, \dots, n$  and  $k = 1, \dots, n$ , define

$$\beta = \min \{ -2r_{i,k}^*, -4\kappa_{i,k}^*, h_{i,k}, \wp_i, \lambda_i, 2m_{i,l}^* \} \quad (61)$$

$$\gamma = \sum_{i=1}^N \sum_{k=1}^n (\iota_{i,k} + \frac{h_{i,k}}{2\eta_{i,k}} W_{i,k}^* W_{i,k}) + \sum_{i=1}^N \left( \sum_{k=1}^{n-1} \frac{\Xi}{2} + \frac{\lambda_i}{2o_i} (\Theta_i^*)^2 \right) \quad (62)$$

To ensure the stability of the entire MASs, it is crucial to appropriately select parameter values while adhering to the following conditions:  $-r_{i,k}^* > 0$ ,  $-\kappa_{i,k}^* > 0$ ,  $h_{i,k} > 0$ ,  $\wp_i > 0$ ,  $\lambda_i > 0$  and  $m_{i,l}^* > 0$ .

Then, one has

$$\dot{V} \leq -\beta V + \gamma \quad (63)$$

When set  $\beta > \gamma/\Delta$ , we get  $\dot{V} < 0$  on  $V = \Delta$ . Further, if at time  $t = 0$  the condition  $V \leq \Delta$  holds, it follows that  $V \leq \Delta$  for entire  $t > 0$ . This demonstrates that the error signals  $z_{i,k}$ ,  $e_{i,k}$ ,  $\tilde{\tau}_{i,k}$ ,  $\tilde{W}_{i,k}$ ,  $\tilde{\Theta}_i$  and  $\psi_{i,k}$  are uniformly bounded. It is straightforward to derive the following:

$$\frac{1}{2} \|\Upsilon_1\|^2 \leq V(t) \leq e^{-\beta t} V(0) + \frac{\gamma}{\beta} (1 - e^{-\beta t}) \quad (64)$$

where  $\Upsilon = [\Upsilon_1^T, \Upsilon_2^T, \dots, \Upsilon_M^T]^T$ . Then, we have  $\|\Upsilon\|^2 \leq 2e^{-\beta t} V(0) + \frac{2\gamma}{\beta} (1 - e^{-\beta t})$ .

Consequently, as time progresses, all consensus tracking errors will converge to a compact set defined as  $\mathfrak{S} = \{\Upsilon_1 | \|\Upsilon_1\| \leq \sqrt{2\gamma/\beta}\}$ . This means that the tracking errors among agents can be modified and reduced to an arbitrarily small range by increasing the parameter  $\beta$ . From (43), one has

$$\dot{\alpha}_i(t) = \dot{w}_{i,n+1} - \frac{\bar{\pi}_i \dot{z}_{i,n}}{\cosh^2\left(\frac{z_{i,n} \bar{\pi}_i}{\mu_i}\right)}. \quad (65)$$

According to [24], one gets

$$\begin{aligned} \frac{d}{dt} |\vartheta_i(t)| &= \frac{d}{dt} (\vartheta_i(t) \times \dot{\vartheta}_i(t))^{\frac{1}{2}} \\ &= \text{sign}(\vartheta_i(t)) \dot{\vartheta}_i(t) \leq |\dot{\vartheta}_i(t)|. \end{aligned} \quad (66)$$

Based on the stability analysis, it is imperative that there exists a positive parameter  $\Pi$  such that  $|\dot{\vartheta}_i(t)| \leq \Pi$ . Based on (41)(42), we have  $\vartheta_i(t_s) = 0$  and  $\lim_{t \rightarrow t_{s+1}} \vartheta_i(t) = \pi_i$ .

Additionally, for the time interval  $t \in [t_s, t_{s+1})$ , the lower bound for the inter-execution time is given by  $t^* \geq \pi_i/\Pi$ .

Following the same analysis in the proof of fixed-threshold strategy, according to (45)(46), the relative-threshold and switch-threshold strategy satisfy  $t^* \geq (\Delta_i |u_i(t)| + \pi_i^*)/\Pi$  and  $t^* \geq \max\{\pi_i, \pi_i^*\}/\Pi$ , respectively. Consequently, the Zeno behaviour is proficiently avoided.

## REFERENCES

- [1] B. V. Solanki, A. Raghurajan, K. Bhattacharya and C. A. Cañizares, "Including Smart Loads for Optimal Demand Response in Integrated Energy Management Systems for Isolated Microgrids," *IEEE Trans Smart Grid*, vol. 8, no. 4, pp. 1739-1748, Jul. 2017.
- [2] F. Perez, G. Damm, C. M. Verrelli and P. F. Ribeiro, "Adaptive Virtual Inertia Control for Stable Microgrid Operation Including Ancillary Services Support," *IEEE Trans. Control Syst. Technol.*, vol. 31, no. 4, pp. 1552-1564, Jul. 2023.
- [3] E. Mousavinejad, F. Yang, Q. -L. Han, X. Ge and L. Vlacic, "Distributed Cyber Attacks Detection and Recovery Mechanism for Vehicle Platooning," *IEEE Trans Intell Transp Syst*, vol. 21, no. 9, pp. 3821-3834, Sept. 2020.
- [4] X. Ge, Q. -L. Han, J. Wang and X. -M. Zhang, "Scalable and Resilient Platooning Control of Cooperative Automated Vehicles," *IEEE Trans. Veh. Technol.*, vol. 71, no. 4, pp. 3595-3608, Apr. 2022.
- [5] W. Li, C. Feng, L. Zhang, H. Xu, B. Cao and M. A. Imran, "A Scalable Multi-Layer PBFT Consensus for Blockchain," *IEEE Trans. Image Process.*, vol. 32, no. 5, pp. 1146-1160, May. 2021.
- [6] A. Pizzo, L. Sanguinetti and T. L. Marzetta, "Fourier Plane-Wave Series Expansion for Holographic MIMO Communications," *IEEE Trans. Wireless Commun.*, vol. 21, no. 9, pp. 6890-6905, Sept. 2022.
- [7] P. Tabuada, "Event-Triggered Real-Time Scheduling of Stabilizing Control Tasks," in *IEEE Trans. Autom. Contrd*, vol. 52, no. 9, pp. 1680-1685, Sept. 2007.
- [8] A. Anta and P. Tabuada, "To Sample or not to Sample: Self-Triggered Control for Nonlinear Systems," *IEEE Trans. Autom. Contrd*, vol. 55, no. 9, pp. 2030-2042, Sept. 2010.
- [9] G. Chen, D. Yao, H. Li, Q. Zhou and R. Lu, "Saturated Threshold Event-Triggered Control for Multiagent Systems Under Sensor Attacks and Its Application to UAVs," *IEEE Trans Circuits Syst I Regul Pap*, vol. 69, no. 2, pp. 884-895, Feb. 2022.
- [10] D. Theodosis and D. V. Dimarogonas, "Event-Triggered Control of Nonlinear Systems With Updating Threshold," *IEEE Contr. Syst. Lett.*, vol. 3, no. 3, pp. 655-660, Jul. 2019.
- [11] X. Wang, Y. Zhou, T. Huang and P. Chakrabarti, "Event-Triggered Adaptive Fault-Tolerant Control for a Class of Nonlinear Multiagent Systems With Sensor and Actuator Faults," *IEEE Trans Circuits Syst I Regul Pap*, vol. 69, no. 10, pp. 4203-4214, Oct. 2022.
- [12] P. Elena, P. Romain, A. Daniele, N. Dragan and H. W. Maurice, "Decentralized event-triggered estimation of nonlinear systems," *Automatica*, vol. 160, pp. 111414, Nov. 2024.
- [13] Z. M. Wang, "Hybrid Event-triggered Control of Nonlinear System with Full State Constraints and Disturbance," *2024 36th Chinese Control and Decision Conference (CCDC)*, pp. 2122-2127, May. 2024.
- [14] R. Postoyan, A. Anta, W. P. M. H. Heemels, P. Tabuada and D. Nešić, "Periodic event-triggered control for nonlinear systems," *52nd IEEE Conference on Decision and Control*, Firenze, Italy, pp. 7397-7402, Dec. 2013.
- [15] L. T. Xing, C. Y. Wen, Z. T. Liu, H. Y. Su, and J. P. Cai, "Event-Triggered Adaptive Control for a Class of Uncertain Nonlinear Systems," *IEEE Trans. Autom. Contrd*, vol. 62, no. 4, pp. 2071-2076, Apr. 2017.
- [16] S. Xiao, X. Ge, Q. -L. Han and Y. Zhang, "Dynamic Event-Triggered Platooning Control of Automated Vehicles Under Random Communication Topologies and Various Spacing Policies," *IEEE Trans. Cybern*, vol. 52, no. 11, pp. 11477-11490, Nov. 2022.
- [17] P. Yu, C. Fischione and D. V. Dimarogonas, "Distributed Event-Triggered Communication and Control of Linear Multiagent Systems Under Tactile Communication," *IEEE Trans. Autom. Contrd*, vol. 63, no. 11, pp. 3979-3985, Nov. 2018.
- [18] C. L. P. Chen, G. X. Wen, Y. J. Liu, and Z. Liu, "Observer-based adaptive backstepping consensus tracking control for high-Order nonlinear semi-strict-feedback multiagent systems," *IEEE Trans. Cybern*, vol. 46, no. 7, pp. 1591-1601, Jul. 2016.
- [19] Z. M. Wang, X. Wang and N. Pang, "Adaptive Fixed-Time Control for Full State-Constrained Nonlinear Systems: Switched-Self-Triggered Case" *IEEE Trans. Circuits Syst. II Express Briefs*, vol. 71, no. 2, pp. 752-756, Feb. 2024.
- [20] N. Pang, X. Wang and Z. M. Wang, "Observer-Based Event-Triggered Adaptive Control for Nonlinear Multiagent Systems With Unknown States and Disturbances," *IEEE Trans. Neural Netw. Learn. Syst*, vol. 34, no. 9, pp. 6663-6669, Sept. 2023.
- [21] S. J. Yoo, "Distributed consensus tracking for multiple uncertain nonlinear strict-feedback systems under a directed graph," *IEEE Trans. Neural Netw. Learn. Syst*, vol. 24, no. 4, pp. 666-672, Apr. 2013.
- [22] L. Liu and X. Li, "Event-Triggered Tracking Control for Active Seat Suspension Systems With Time-Varying Full-State Constraints," *IEEE Trans. Syst. Man Cybern. Syst.*, vol. 52, no. 1, pp. 582-590, Jan. 2022.
- [23] Z. M. Wang, H. Wang, X. Wang, N. Pang and Q. Shi, "Event-Triggered Adaptive Neural Control for Full State-Constrained Nonlinear Systems with Unknown Disturbances" *Cognit. Comput.*, vol. 16, no. 2, pp. 717-726, Dec. 2023.
- [24] T. Henningsson, E. Johannesson, and A. Cervin, "Sporadic event-based control of first-order linear stochastic systems," *Automatica*, vol. 44, no. 11, pp. 2890-2895, Nov. 2008.